Numer. Math. 70: 379–396 (1995)

Numerische
Mathematik

Wavelet solutions for the Dirichlet problem*

Raymond O. Wells, Jr., Xiaodong Zhou

Rice University, Houston, Texas, USA

Received June 3, 1992 / Revised version received November 8, 1993

Summary. A modified classical penalty method for solving a Dirichlet boundary value problem is presented. This new *fictitious domain penalty* method eliminates the traditional need of generating a complex computation grid in the case of irregular domains. It is based on the fact that one can expand the *boundary measure* under the chosen basis which leads to a fast, approximate calculation of boundary integral. The compact support and orthonormality of the basis are essential for representing the boundary measure numerically, and therefore for implementing this methodology.

Mathematics Subject Classification (1991): 65N30

1. Introduction

Compactly supported wavelets which are differentiable were introduced by Daubechies in her celebrated paper [2], which has had applications in a number of areas. Since these functions combine orthogonality with localization and scaling properties it has been a natural idea to attempt to use these functions for the numerical approximation to solutions to partial differential equations. There have been a number of papers in this direction including studies of Burgers' equation ([7], [11], and [12]) as well as two-dimensional turbulent flow [14]. In these papers the boundary conditions are imposed by using primarily periodic boundary conditions, and looking at the behavior of the solution as a function of time. Another point of view was introduced in [13] in which the boundary, the boundary data, and the unknown solution (of a boundary value problem) on the interior of a domain are all uniformly represented in terms of compactly supported wavelet functions in an extrinsic ambient Euclidean space. This is similar to the spectral method in solving differential equations (essentially using an orthonormal expansion), but here we use the localization property of wavelets to extend this orthonormal representation to boundary data and geometric boundaries.

In this paper we illustrate this principle with an application to the Dirichlet problem for a classical elliptic differential equation. There are several parts to this implemen-

* This research has been supported by AFOSR under Grant No. 90-0334, which was funded by DARPA, and by Aware, Inc

tation which require some preliminary explanation. We consider a classical elliptic boundary value problem, with a differential equation of the form:

$$\begin{aligned} -\Delta u + u &= f \text{ in } \omega, \\ u|_{\partial\omega} &= g, \end{aligned} \tag{1.1}$$

where ω is a bounded domain in $\mathbf{R}^n$, with a boundary satisfying a suitable regularity condition. The basic principle divides into three basic points:

1. Represent the geometric region for the boundary value problem in terms of wavelets. For this we use the characteristic function of the domain χ_ω and let $\nabla\chi_\omega$ represent its boundary as a measure on $\mathbf{R}^n$. Both of these functions can be represented in terms of a wavelet series, using differentiable wavelets and the connection coefficients which are useful for calculating derivatives of wavelet expansions (see [1], [10]).
2. Represent the functions defined on the boundary and on the interior of the region in terms of wavelet series defined in a rectangular region containing the domain. For this we observe that approximate solutions of differential equations are restrictions of functions defined on all of $\mathbf{R}^n$, while any function defined on the boundary in some smoothness class admits extensions (not unique) to the ambient space. Hence we can consider ambient functions defined in terms of a wavelet series and their restriction to the boundary (in the sense we prescribe below) to be valid representations for boundary data for the problem.
3. Convert the differential equation to some weak form, involving integration over the interior and along the boundary, all of which are to be represented in terms of wavelets (as in [13], where an example of this type of integration was carried out).
4. Formulate and solve a wavelet-Galerkin problem for the domain and the differential equation, using localized wavelets as an orthonormal basis, and representing both the unknown functions and the test functions in terms of the same basis.

This process is carried out in this paper using Daubechies wavelets with 6 coefficients (which are barely first-order differentiable), and for a particular weak formulation, based on a penalty method, as in [6], Appendix 1. It works quite well as we see in both the convergence proofs presented below as well as in the confirming numerical experiments.

One important property of this numerical scheme is that the coding for the solution of the boundary value problem is *independent* of the geometry of the boundary. The geometry of the boundary is encoded in the scanning and digitizing at the pixel scale of the geometric region under consideration; this is a simple input to the problem, and it can be changed as simply as the boundary data itself can be changed. Normally in finite element approaches to such a boundary value problem one has a finite element grid which is *adapted* to the boundary. This is not necessary for this scheme which gives it great flexibility in applications.

One presumably can use any basis functions to implement the idea presented in this paper. However, under the finite element basis, the approximation of *boundary measure* (see Sect. 3.2) is not as good as the one in terms of wavelet basis, one possible reason may be that finite element basis is not orthonormal. See [8] for relative discussions, and a comparison of wavelet and finite element methods.

In this paper we formulate all of the theoretical results in two dimensions, although we could easily have expressed them in arbitrary dimensions. In Sect. 2.1 we give a

review and a summary of the basic information about wavelets which we need for this paper. In Sect. 3.1 we exhibit explicitly and give some of the theoretical background for the geometric-measure theoretic objects which play a major role in this paper. This includes arc-length (more generally surface measure in the higher-dimensional case), integrals of differential forms over the oriented boundary of the given domain $\partial\omega$, as well as Radon measures representing integration of a function over the same boundary. In Sect. 3.2 we find wavelet representations of these same objects, using the characteristic function of the domain as the principal way in which the geometry is expressed. We show that natural truncations of these wavelet representation formulas (used in the experiments) converge at specific and calculable rates. Finally, in Sect. 4 we formulate the Dirichlet problem we want to solve. We give a weak form of this, and convert it to a fictitious domain problem (embedding our given domain in a bigger rectangular domain). We formulate a wavelet-Galerkin solution for this problem, and prove convergence theorems for these numerical approximation schemes.

The numerical experiments for the Dirichlet problem are described in Section 5.4. In the penalty method approach to solving the Dirichlet problem, employed in Sect. 5, one finds a numerical approximation u_ϵ^j to a regularized approximation u_ϵ of the solution to the Dirichlet problem. As we see in Sect. 5.3 we have an estimate of the form (among others)

$$\|u_\epsilon^j - u\|_{L^2(\omega)} = o(1) + O(2^{-2j}).$$

We ran a sequence of experiments with varying values of ϵ ($\epsilon = 1$ to $\epsilon = 10^{-12}$) and measured the relative error

$$E := \frac{\|u_\epsilon^j - u\|_{L^2(\omega)}}{\|u\|_{L^2(\omega)}},$$

for a number of different geometries of ω and a number of different exact solutions to one equation. For instance, for the exact solution $u = x^2 + y^2$ on the disk and the diamond (with corners, but not aligned with the translation axes), one finds relative errors of the order of 10^{-7} for $\epsilon = 10^{-12}$, for a fixed wavelet size of support length 5 versus a diameter of the diamond of 10. The fictitious domain Ω had a diameter of 30. These feasibility studies show that this method works quite well, gives good accuracy, and, most importantly, the coding is *independent* of the geometry of the domain ω on which the boundary value problem is being solved. The geometric data for the boundary is "scanned in" in the same way that the boundary data is "scanned in".

2. Wavelet analysis

2.1. Daubechies wavelets

In this section we will briefly recall the Daubechies compactly supported wavelets which are differentiable and which will be used in this paper ([2], [3]). Let N be a positive integer, and consider a $2 \times 2N$ matrix of the form

$$A = \begin{pmatrix} a_0^0 & \cdots & a_{2N-1}^0 \\ a_0^1 & \cdots & a_{2N-1}^1 \end{pmatrix}, \tag{2.2}$$

where

$$\sum_{k=0}^{2N-1} a_k^r a_{k+2l}^s = 2\delta_{l,0}\delta^{r,s}, \tag{2.3}$$

$$\sum_{k=0}^{2N-1} a_k^r = 2\delta^{r,0}, \tag{2.4}$$

where

$$\delta^{l,m} = \delta_{l,m} = \begin{cases} 0 & l \neq m \\ 1 & l = m, \quad l, m \in \mathbf{Z} \end{cases}$$

is the Kronecker delta function. This is a *wavelet matrix* of *rank* 2 and *genus* N (see [9]). We assume, without loss of generality, that

$$a_k^1 = (-1)^{k+1} a_{2N-1-k}^0,$$

and consider $\phi(x)$ and $\psi(x)$ defined by:

$$\phi(x) = \sum_{k=0}^{2N-1} a_k^0 \phi(2x-k),$$

$$\psi(x) = \sum_{k=0}^{2N-1} a_k^1 \phi(2x-k).$$

The function $\phi(x)$ is called the *scaling function* associated with A, and $\psi(x)$ is called the *wavelet function* associated with A. The dilations and translations of ϕ and ψ are defined as

$$\phi_k^j(x) := 2^{\frac{j}{2}} \phi(2^j x - k),$$

$$\psi_k^j(x) := 2^{\frac{j}{2}} \psi(2^j x - k), \tag{2.5}$$

where $k \in \mathbf{Z}$, $j \in \mathbf{Z}^+$ (the nonnegative integers).

We now list some of the important properties of the Daubechies wavelet system of genus N (which will be the only wavelet systems used in this paper):

$$\int_{\mathbf{R}} \phi(x)dx = 1,$$

$$\sum_{k\in\mathbf{Z}} \phi_k(x) = 1, \tag{2.6}$$

$$\int_{\mathbf{R}} x^m \psi(x)dx = 0, \quad m = 0, \ldots, N-1,$$

$$\text{supp } \phi_k^j = \text{supp } \psi_k^j = \left[\frac{k}{2^j}, \frac{k+2N-1}{2^j}\right] \tag{2.7}$$

Moreover, if we define

$$V_j := L^2\text{-closure}\,(\text{span}\left\{\phi_k^j : k \in \mathbf{Z}\right\}), \tag{2.8}$$

then

$$\bigcup_{j\in\mathbf{Z}} V_j = L^2(\mathbf{R}), \tag{2.9}$$

in the sense that

$$\lim_{j\to\infty} P_j f = f, \tag{2.10}$$

where P_j is the L^2 orthogonal projection from $L^2(\mathbf{R})$ to V_j.

3. Wavelet representation of geometric domains

3.1. Elements of geometric measure theory

In this subsection, we will briefly review some basic measure-theoretic properties concerning sets of finite perimeter. Readers are referred to [4] or [5] for more details on geometric measure theory. The properties developed will include specific formulas from geometric measure theory for boundary integrals and related quantities. In the next section we will represent these same quantities in terms of wavelets.

We will say that a Lebesgue integrable function u is of *bounded variation* over a domain $U \subset \mathbf{R}^2$ if

$$\sup_{g\in C_0^1(U,\mathbf{R}^2),|g|\le 1} \int_U u\mathrm{div} g\, dxdy \le +\infty.$$

Suppose that u is of bounded variation in $U \subset \mathbf{R}^2$. Then, using the Reisz representation theorem, there exist a Radon measure μ and a μ-measurable function ν with $|\nu(x, y)| = 1$, for μ-almost every $(x, y) \in U$, so that, for any $g \in C_0^1(U, \mathbf{R}^2)$,

$$\int_U u\mathrm{div} g\, dxdy = \int_U g \cdot \nu\, d\mu.$$

We will denote by $|\nabla u|$ the Radon measure μ and by ∇u the vector-valued measure $\nu\cdot\mu$. Note that if u is continuously differentiable, then μ is the 2-dimensional Lebesgue measure weighted by the norm of the gradient of u and $\nu = \dfrac{\nabla u}{|\nabla u|}$.

We will say that an open set ω is of *finite perimeter in* U if its characteristic function χ_ω is of bounded variation in U. In particular, we say ω is of *finite perimeter* if χ_ω is a function of bounded variation in $\mathbf{R}^2$.

Proposition 3.1. *For any open set U, if ω is of finite perimeter in U, then*

$$\int_U |\nabla\chi_\omega| = \sup_{g\in C_0^1(U,\mathbf{R}^2),|g|\le 1} \int_\omega \mathrm{div} g\, dxdy. \tag{3.1}$$

In particular, if $\partial\omega$ is piecewise smooth, then

$$\int_U |\nabla\chi_\omega| = l(\partial\omega \cap U). \tag{3.2}$$

(Here $l(\partial\omega \cap U)$ is the arclength of $\partial\omega$ inside U.)

Again, by the Reisz representation theorem, there exists a vector-valued $|\nabla\chi_\omega|$-measurable function ν with $|\nu| = 1$, $|\nabla\chi_\omega|$-almost everywhere. In the case that $\partial\omega$ is a level set of some Lipschitz function F, then $\nu = \dfrac{\nabla F}{|\nabla F|}$ almost everywhere along the boundary $\partial\omega$ and $\int \nu \cdot \nabla\chi_\omega$ is the arclength of $\partial\omega$.

Assume ω is a bounded domain in $\mathbf{R}^2$ whose boundary $\partial\omega$ admits a representation of the form

$$\partial\omega = \{(x, y) \in \mathbf{R}^2 : \quad F(x, y) = c\}$$

for some Lipschitz function F and constant c. Then the unit normal vector along the boundary $\partial\omega$, $\mathbf{n}$, can be written as

$$\mathbf{n} = \frac{\nabla F}{|\nabla F|}. \tag{3.3}$$

Hence by extending $\mathbf{n}$ to $\mathbf{R}^2$ "smoothly", we formally derive the following formula for the arclength of $\partial\omega$,

$$\begin{aligned} l(\partial\omega) \quad &:= \quad \int_{\partial\omega} ds = \int_{\partial\omega} \mathbf{n} \cdot \mathbf{n}\, ds = \int_{\omega} \mathrm{div}\mathbf{n}\, dxdy \\ &= \quad \int_{\mathbf{R}^2} \chi_\omega \mathrm{div}\mathbf{n}\, dxdy = -\int_{\mathbf{R}^2} \nabla\chi_\omega \cdot \mathbf{n}\, dxdy, \end{aligned}$$

where χ_ω is the characteristic function of ω. So we have

$$l(\partial\omega) = -\int_{\mathbf{R}^2} \nabla\chi_\omega \cdot \mathbf{n}\, dxdy. \tag{3.4}$$

More generally, by the same derivation, one has for any integrable function f defined on $\partial\omega$, after extending f to $\mathbf{R}^2$,

$$\int_{\partial\omega} f\, ds = -\int_{\mathbf{R}^2} f\, ||\partial\omega||, \tag{3.5}$$

where we use $||\partial\omega||$ to denote this boundary measure defined as

$$\|\partial\omega\| := -\nabla\chi_\omega \cdot \mathbf{n}. \tag{3.6}$$

3.2. A wavelet approximation of geometric measure integrals

Let ω be an open bounded set in $\mathbf{R}^2$ whose boundary is defined by

$$\partial\omega = \{(x, y) \in \mathbf{R}^2 : F(x, y) = t\},$$

for some Lipschitz function F defined in $\mathbf{R}^2$ and for some constant t. It follows that ω has finite perimeter and all of the analysis in Sect. 3.1 is valid. In addition, let $\{\phi_k^j(x), \psi_k^j(x)\}$ be a Daubechies wavelet system of genus N in $\mathbf{R}$.

We can sample the characteristic function χ_ω and the defining function F in terms of scaling functions at a certain level j as follows:

$$\chi_\omega^j(x, y) := \sum_{p,q} \chi_{p,q}^j \phi_p^j(x) \phi_q^j(y), \tag{3.7}$$

$$F^j(x,y) := \sum_{p,q} F^j_{p,q}\phi^j_p(x)\phi^j_q(y), \tag{3.8}$$

where $\chi^j_{p,q} = \frac{1}{2^j}\chi_\omega(\frac{p+c}{2j}, \frac{q+c}{2j})$, and $F^j_{p,q} = \frac{1}{2^j}F(\frac{p+c}{2j}, \frac{q+c}{2j})$, with $c := \int x\phi(x)dx$. We note that in the wavelet expansions (3.7) and (3.8) the coefficients are given by sampling. This is not the case for many of the expansions used below (see e.g. (3.9), (3.17), and (3.16)).

Remark. If F is C^2, then by [15], F^j will converge to F in $H^1(\omega)$ as $j \to +\infty$. In fact, by a little more careful analysis, we can prove the following

Theorem 3.2. *Assume ω is a bounded set of finite perimeter in $\mathbf{R}^2$, then χ^j_ω (3.7) converges to χ_ω in $L^2(\mathbf{R}^2)$ as $j \to +\infty$.*

Proof. Since ω is bounded, then $\chi_\omega \in L^2(\mathbf{R}^2)$. Let us set for $j \in \mathbf{Z}$,

$$P_j\chi_\omega(x,y) := \sum_{p,q} \tilde{\chi}^j_{p,q}\phi^j_p(x)\phi^j_q(y), \tag{3.9}$$

the L^2-projection of χ_ω into V_j where

$$\tilde{\chi}^j_{p,q} = \int_{\mathbf{R}^2} \chi_\omega(x,y)\phi^j_p(x)\phi^j_q(y)\,dxdy.$$

Then by (2.10), we have that

$$||P_j\chi_\omega - \chi_\omega||_{L^2(\mathbf{R}^2)} \to 0, \qquad \text{as } j \to +\infty. \tag{3.10}$$

Thus to prove the theorem, it is sufficient to show that

$$||P_j\chi_\omega - \chi^j_\omega||_{L^2(\mathbf{R}^2)} \to 0, \quad \text{as } j \to +\infty. \tag{3.11}$$

Setting the index set $\Lambda^j_\omega = \{(p,q) \in Z \times Z : \text{supp}\,(\phi^j_p(x)\phi^j_q(y)) \cap \partial\omega \neq \emptyset.\}$. Then, we have

$$P_j\chi_\omega - \chi^j_\omega = \sum_{\{p,q\}\in\Lambda^j_\omega} w^j_{p,q}\phi^j_p(x)\phi^j_q(y), \tag{3.12}$$

where

$$w^j_{p,q} := \int_{\mathbf{R}^2} \left(\chi_\omega\left(\frac{p+c}{2j}, \frac{q+c}{2j}\right) - \chi_\omega(x,y)\right)\phi^j_p(x)\phi^j_q(y)\,dxdy. \tag{3.13}$$

Hence

$$||P_j\chi_\omega - \chi^j_\omega||^2_{L^2(\mathbf{R}^2)} = \sum_{\{p,q\}\in\Lambda^j_\omega} w^2_{p,q}. \tag{3.14}$$

On the other hand, using the Hölder inequality and (2.6),

$$\begin{aligned} w^2_{p,q} &\leq \left(\int |\phi^j_p(x)|\,dx\right)^2 \left(\int |\phi^j_q(y)|\,dy\right)^2 \\ &\leq |\text{supp}\,(\phi^j_p(x))||\text{supp}\,(\phi^j_q(y))| \\ &\leq C(N)\left(\frac{1}{2^j}\right)^2, \end{aligned}$$

where $C(N)$ is a constant which depends on N, and for any set S, $|S|$ denotes its Lebesgue measure. Therefore, from (3.14), we derive

$$||P_j\chi_\omega - \chi_\omega^j||^2_{L^2(\mathbf{R}^2)} \le C(N)\ \text{card}(\Lambda_\omega^j)/2^{2j}, \tag{3.15}$$

here, we use card (Λ_ω^j) to denote the cardinality of the index set Λ_ω^j. To estimate this cardinality, we notice that $\cup_{\Lambda_\omega^j} \text{supp}(\phi_p^j(x)\phi_q^j(y)) \subset U^j$, where U_ω^j is the tubular neighborhood of $\partial\omega$ of width $2\sqrt{2}/2^j$. Also, for each point in U_ω^j, the number of squares in the union containing this point is bounded by a constant depending only on N. Therefore

$$C(N)\text{card}(\Lambda_\omega^j)(\frac{1}{2^j})^2 \le \text{area}(U_\omega^j) \le l(\partial\omega)C_1(N)\frac{1}{2^j}, \tag{3.16}$$

where $l(\partial\omega)$ should be understood as $\int_{\mathbf{R}^2} |\nabla\chi_\omega| dxdy$ for general domains of finite perimeter. This implies

$$\text{card}(\Lambda_\omega^j) \le C(N,\omega)2^j,$$

where $C(N,\omega)$ is a constant depending on N and ω. Combining this with (3.15), the theorem is proved. □

By differentiating the right hand sides of (3.7) and (3.8), and using the connection coefficients defined by (see [1], [10]) for a discussion of connection coefficients)

$$\Gamma_m^l := \int_{\mathbf{R}} \phi_l'\phi_m\, dx,$$

one derives the expansions for the partial derivatives of χ_ω and F,

$$\frac{\partial\chi_\omega^j}{\partial x}(x,y) = \sum_{p.q}\left(\frac{\partial\chi}{\partial x}\right)_{p,q}^j \phi_p^j(x)\phi_q^j(y), \tag{3.17}$$

$$\frac{\partial\chi_\omega^j}{\partial y}(x,y) = \sum_{p.q}\left(\frac{\partial\chi}{\partial y}\right)_{p,q}^j \phi_p^j(x)\phi_q^j(y), \tag{3.18}$$

$$\frac{\partial F^j}{\partial x}(x,y) = \sum_{p.q}\left(\frac{\partial F}{\partial x}\right)_{p,q}^j \phi_p^j(x)\phi_q^j(y), \tag{3.19}$$

$$\frac{\partial F^j}{\partial y}(x,y) = \sum_{p.q}\left(\frac{\partial F}{\partial y}\right)_{p,q}^j \phi_p^j(x)\phi_q^j(y), \tag{3.20}$$

where, for example, the coefficients in (3.17) are of the form:

$$\left(\frac{\partial\chi}{\partial x}\right)_{p,q}^j = \sum_m \Gamma_m^p\chi_{m,q}^j.$$

By Theorem 3.2, we have the following

Corollary 3.3. *Under the assumption in Theorem* 3.2, $\nabla\chi_\omega^j$ *converges to* $\nabla\chi_\omega$ *(as distributions), as* $j \to +\infty$, *and the support of* $\nabla\chi_\omega^j$ *is contained in* U_ω^j.

Proof. For $N \geq 3$, the scaling function ϕ is differentiable, hence for any continuously differentiable vector-valued function $\boldsymbol{\xi}$, using integration by parts, one has

$$\int \boldsymbol{\xi} \cdot \nabla \chi_\omega^j \, dxdy = \int \operatorname{div}(\boldsymbol{\xi}) \chi_\omega^j \, dxdy.$$

Then the corollary follows readily from Theorem 1 by letting $j \to +\infty$. The second conclusion in the corollary is obvious. □

Now we approximate the normal vector **n** at level j by

$$n_x^j(x,y) := \sum_{p,q} \frac{\left(\frac{\partial F}{\partial x}\right)_{p,q}^j}{|\nabla F|_{p,q}^j} \phi_p^j(x) \phi_q^j(y). \tag{3.21}$$

and

$$n_y^j(x,y) := \sum_{p,q} \frac{\left(\frac{\partial F}{\partial y}\right)_{p,q}^j}{|\nabla F|_{p,q}^j} \phi_p^j(x) \phi_q^j(y) \tag{3.22}$$

with $\mathbf{n}^j = (n_x^j, n_y^j)$, where

$$|\nabla F|_{p,q}^j := \sqrt{\left(\left(\frac{\partial F}{\partial x}\right)_{p,q}^j\right)^2 + \left(\left(\frac{\partial F}{\partial y}\right)_{p,q}^j\right)^2}.$$

Lemma 3.4. *Assume that F is twice differentiable, then $\mathbf{n}^j$ converges to* **n** *in $H^1_{\mathrm{loc}}(\mathbf{R}^2)$ as $j \to +\infty$.*

Proof. Use the continuity of ∇F. □

Using the formula (3.6), and taking (3.17), (3.18), (3.21) and (3.22) into account, we approximate the boundary measure $\|\partial\omega\|$ at level j by

$$\|\partial\omega\|^j := \sum_{p,q} \mu_{p,q}^j \phi_p^j(x) \phi_q^j(y).$$

Where

$$\mu_{p,q}^j = -\left[\left(\left(\frac{\partial \chi}{\partial x}\right)_{p,q}^j \left(\frac{\partial F}{\partial x}\right)_{p,q}^j + \left(\frac{\partial \chi}{\partial y}\right)_{p,q}^j \left(\frac{\partial F}{\partial y}\right)_{p,q}^j\right) / |\nabla F|_{p,q}^j\right]. \tag{3.23}$$

Then

$$l^j(\partial\omega) := \frac{1}{2^j} \sum_{p,q} \mu_{p,q}^j$$

should approximate the arc length of $\partial\omega$. Indeed, we have the following

Theorem 3.5. *Suppose ω is a bounded set of finite perimeter, and that the function F is twice differentiable, then $l^j(\partial\omega)$ converges to the length of $\partial\omega$ as $j \to +\infty$.*

Proof. It follows directly from Corollary 3.2 and Theorem 3.1. □

For a more general domain, we also have the following

Theorem 3.6. *Assume that $\partial\omega$ is Lipschitz and piecewise smooth with a finite number of nonsmooth points. Then, as $j \to +\infty$, $l^j(\partial\omega)$ converges to $l(\partial\omega)$, the length of $\partial\omega$.*

Proof. For any function $g \in C_0^1(\mathbf{R}^2, \mathbf{R}^2)$, by the definition of χ_ω^j, one has

$$\int_{\mathbf{R}^2} \chi_\omega^j \mathrm{div} g \, dxdy = \int_{\omega^j} \mathrm{div} g \, dxdy, \tag{3.24}$$

where $\omega^j = \cup_{p,q\in I^j} \mathrm{supp}(\phi_p^j(x)\phi_q^j(y))$, and $I^j = \{(p,q) : \mathrm{supp}(\phi_p^j(x)\phi_q^j(y)) \cap \omega \neq \emptyset\}$. Hence by Proposition 2.1 in Sect. 1.4, one has

$$\int_{\mathbf{R}^2} |\nabla \chi_\omega^j| \, dxdy \leq \int_{\mathbf{R}^2} |\nabla \chi_{\omega^j}|. \tag{3.25}$$

In fact, using the same derivation, one has (3.25) for any open set $U \subset \mathbf{R}^2$. That is,

$$\int_U |\nabla \chi_\omega^j| \, dxdy \leq \int_U |\nabla \chi_{\omega^j}|. \tag{3.26}$$

By definition,

$$l^j(\partial\omega) = \int_{\mathbf{R}^2} \mathbf{n}^j \cdot \nabla \chi_\omega^j \, dxdy, \tag{3.27}$$

and

$$l(\partial\omega) = \int_{\mathbf{R}^2} \mathbf{n} \cdot \nabla \chi_\omega \, dxdy. \tag{3.28}$$

We call the nonsmooth points of $\partial\omega$ *corners*, and we note that, under the assumptions on ω, $\mathbf{n}^j \to \mathbf{n}$ strongly in the H^1 norm on any subset not including the corners. We note that the wavelet expansion is localized because of the compact support of the wavelets. For any small positive number ϵ, one can choose an open set V containing all the corners so that

$$l(\partial\omega \cap V) < \epsilon.$$

Then, as in the proof of Theorem 1,

$$\int_{\mathbf{R}^2 - \bar{V}} \mathbf{n}^j \cdot \nabla \chi_\omega^j \to \int_{\mathbf{R}^2 - \bar{V}} \mathbf{n} \cdot \nabla \chi_\omega, \quad \text{as } j \to +\infty. \tag{3.29}$$

On the other hand, $|\int_V \mathbf{n} \cdot \nabla \chi_\omega| \leq l(\partial\omega \cap V) < \epsilon$. To estimate $|\int_V \mathbf{n}^j \cdot \nabla \chi_\omega^j|$, recalling (3.17) and (3.18), one has in fact that

$$\mathrm{card}(\Lambda_V^j) \leq C(N) l(\partial\omega \cap V) 2^j,$$

where $\Lambda_V^j = \{(p,q) : \quad \mathrm{supp}(\phi_p^j(x)\phi_q^j(y)) \cap V \neq \emptyset\}$. Therefore, by (3.26),

$$\begin{aligned} \left| \int_V \mathbf{n}^j \cdot \nabla \chi_\omega^j \right| &\leq \int_V |\nabla \chi_{\omega^j}| \\ &= l(\partial\omega^j \cap V) \leq C(N) \mathrm{card}(\Lambda_V^j) \frac{1}{2^j} \\ &\leq C(N) l(\partial\omega \cap V) \leq C(N)\epsilon. \end{aligned} \tag{3.30}$$

hence, by (3.29) and (3.30), the theorem is proved. □

The approximation of the boundary integral of a function f over $\partial\omega$ now can be obtained through (3.5) in a straightforward manner. Namely,

$$\int_{\partial\omega} f\,ds \approx \int_{\mathbf{R}^2} f^j \|\partial\omega\|^j. \tag{3.31}$$

In general, one needs some technical assumptions on both f and $\partial\omega$ to prove the right hand side of (3.31) indeed converges to the boundary integral. For instance, if f is a restriction of a function smooth in the neighborhood of $\partial\omega$ and $\partial\omega$ is Lipschitz, then one has the desired convergence.

4. The Dirichlet problem

4.1. A fictitious domain penalty formulation

Let ω be a Lipschitz domain in $\mathbf{R}^2$ and functions $f \in L^2(\omega), g \in H^{\frac{1}{2}}(\partial\omega)$ be given. We consider a Dirichlet problem of the form: find $u \in H^1(\omega)$, so that

$$\begin{aligned} -\triangle u + u &= f, \qquad \text{in } \omega, \\ u &= g, \qquad \text{on } \partial\omega. \end{aligned} \tag{4.1}$$

To solve the above problem using finite difference or finite element methods in the case of an irregular geometric domain, one difficult task is to generate a complex grid adapted to the geometry of ω, which is very time-consuming. Here we propose a formulation which enables us to work with a regular mesh grid. More specifically, we solve a penalty problem [6] in a slightly larger, but simply shaped (rectangular in general) domain Ω.

Let Ω be a square containing ω. For $\epsilon > 0$, find $u_\epsilon \in H^1_{\mathrm{p}}(\Omega)$, so that

$$\int_\Omega \nabla u_\epsilon \cdot \nabla v + u_\epsilon v \frac{1}{\epsilon} \int_{\partial\omega} u_\epsilon v\,ds = \int_\Omega \tilde{f} v + \frac{1}{\epsilon} \int_{\partial\omega} g v\,ds, \tag{4.2}$$

for any $v \in H^1_{\mathrm{p}}(\Omega)$, where $H^1_{\mathrm{p}}(\Omega)$ is the space of H^1 functions in Ω which are periodic in x and y. Here $\tilde{f}$ is an arbitrary L^2 extension of f to Ω. Clearly, u_ϵ exists for every $\epsilon > 0$. In the next section, we modify the proof of Proposition 4.14 in [6] to show that u_ϵ converges to a function u whose restriction to ω is the desired solution.

4.2. Convergence of the solution of the penalized problem

Theorem 4.1. *Let u_ϵ be the solution of* (4.2)*, and u be the solution of* (4.1)*. Then*

$$||u_\epsilon - u||_{H^1(\omega)} \to 0, \qquad \textit{as } \epsilon \to 0 \tag{4.3}$$

Proof. We follow the proof of Proposition 4.14 in [6]. Let us first consider the variational problem: find $\tilde{u} \in V_g$ so that

$$\int_\Omega \nabla\tilde{u} \cdot \nabla v \, dxdy + \int_\Omega \tilde{u} v \, dxdy = \int_\Omega f v \, dxdy, \quad \forall v \in V_0, \tag{4.4}$$

where

$$\begin{aligned} V_0 &= \{v : v \in H^1_p(\Omega), \quad v = 0 \text{ on } \partial\omega\}, \\ V_g &= \{v : v \in H^1_p(\Omega), \quad v = g \text{ on } \partial\omega\}. \end{aligned}$$

Since $g \in H^{\frac{1}{2}}(\partial\omega)$, the affine space V_g is not empty, which implies that problem (4.4) has a unique solution. Taking v successively with compact support in ω and $\Omega - \bar{\omega}$ we see that the solution $\tilde{u}$ of (4.4) satisfies

$$\begin{aligned} -\Delta\tilde{u} + \tilde{u} &= f \text{ in } \omega, \quad \tilde{u} = g \text{ on } \partial\omega, \\ -\Delta\tilde{u} + \tilde{u} &= f \text{ in } \Omega - \bar{\omega}, \quad \tilde{u} = g \text{ on } \partial\omega, \qquad \frac{\partial\tilde{u}}{\partial n} = 0 \text{ on } \partial\Omega. \end{aligned} \tag{4.5}$$

The function $\tilde{u}\,|_\omega$ coincides therefore with the solution u of (4.1). Take now $v = u_\epsilon - \tilde{u}$ in (4.2), and we find that

$$\begin{aligned} &\int_\Omega \nabla u_\epsilon \cdot (u_\epsilon - \tilde{u}) \, dxdy + \int_\Omega u_\epsilon (u_\epsilon - \tilde{u}) \, dxdy + \frac{1}{\epsilon} \int_{\partial\omega} u_\epsilon (u_\epsilon - \tilde{u}) \, ds \\ &= \int_\Omega f(u_\epsilon - \tilde{u}) \, dxdy + \frac{1}{\epsilon} \int_{\partial\omega} g(u_\epsilon - \tilde{u}) \, ds, \end{aligned}$$

which implies

$$\begin{aligned} &\int_\Omega |\nabla(u_\epsilon - \tilde{u})|^2 \, dxdy + \int_\Omega |(u_\epsilon - \tilde{u})|^2 \, dxdy + \frac{1}{\epsilon} \int_{\partial\omega} |(u_\epsilon - \tilde{u})|^2 \, ds \\ &= \int_\Omega f(u_\epsilon - \tilde{u}) \, dxdy - \int_\Omega \nabla\tilde{u} \cdot \nabla(u_\epsilon - \tilde{u}) \, dxdy - \int_\Omega \tilde{u}(u_\epsilon - \tilde{u}) \, dxdy. \end{aligned} \tag{4.6}$$

By Cauchy's inequality, it follows from (4.5) that

$$\|u_\epsilon - \tilde{u}\|_{H^1(\Omega)} \leq C. \tag{4.7}$$

where C is independent of ϵ. Therefore (4.7) and weak compactness of the unit ball in $H^1(\Omega)$ imply that one can extract from $\{u_\epsilon\}$ a subsequence (which we continue to denote by $\{u_\epsilon\}$ for simplicity) converging weakly to an element u^* of $H^1(\Omega)$. Since the mapping from $H^1(\Omega)$ to $L^2(\partial\omega)$ is in fact compact, it follows that $u_\epsilon\,|_{\partial\omega}$ converges strongly to $u^*\,|_{\partial\Omega}$ in $L^2(\partial\omega)$. On the other hand, from the uniform boundedness of u_ϵ in the space $H^1(\Omega)$ (see (4.7)), (4.6) implies that $u_\epsilon\,|_{\partial\omega}$ converges strongly to g in $L^2(\partial\omega)$. Hence,

$$u^* = g \text{ on } \partial\omega \tag{4.8}$$

To show that $u^* = \tilde{u}$, take $v \in V_0$ in (4.2); we have then

$$\int_\Omega \nabla u_\epsilon \cdot v \, dxdy + \int_\Omega u_\epsilon v \, dxdy = \int_\Omega f v \, dxdy, \quad \forall v \in V_0. \tag{4.9}$$

Taking the limit in (4.9) as $\epsilon \to 0$ it follows from the weak $H^1(\Omega)$-convergence of u_ϵ to u^* that

$$\int_\Omega \nabla u^* \cdot \nabla v \, dxdy + \int_\Omega u^* v \, dxdy = \int_\Omega f v \, dxdy, \forall v \in V_0. \tag{4.10}$$

Combining (4.10) and (4.8) shows that $u^* = \tilde{u}$, and therefore, since problem (4.4) has a unique solution it is the *whole sequence* $\{u_\epsilon\}$ which converges to $\tilde{u}$. Finally, to show the strong convergence of u_ϵ to $\tilde{u}$ in $H^1(\Omega)$, observe that (4.6) implies that

$$\begin{aligned} \|u_\epsilon - \tilde{u}\|^2_{H^1(\Omega)} \quad \leq \quad & \int_\Omega f(u_\epsilon - \tilde{u}) \, dxdy - \int_\Omega \nabla \tilde{u} \cdot \nabla (u_\epsilon - \tilde{u}) \, dxdy \\ & - \int_\Omega \tilde{u}(u_\epsilon - \tilde{u}) \, dxdy. \end{aligned} \tag{4.11}$$

The weak $H^1(\Omega)$-convergence of u_ϵ to $\tilde{u}$ implies that the right hand side of (4.11) converges to 0 as $\epsilon \to 0$, which implies in turn that $\lim_{\epsilon \to 0} \|u_\epsilon - \tilde{u}\|_{H^1(\Omega)} = 0$; by restriction to ω we obtain the strong convergence of $u_\epsilon \mid_\omega$ to u in $H^1(\omega)$. □

4.3. The wavelet-Galerkin approximation

For simplicity, let us assume the square $\Omega = (0, s)^2$, s is an integer. For $l = \mathbf{Z}^+$, we set

$$V_{\mathrm{P}}^l = V_{\mathrm{P}}^l(0, s) := \left\{ v \in L^2(0, s) : v(x) = \sum_{k \in \mathbf{Z}} c_k \phi_k^l(x), \quad x \in (0, s), \quad \text{with } c_k = c_{k+2^l s} \right\},$$

and we use

$$X_{\mathrm{P}}^l = V_{\mathrm{P}}^l \otimes V_{\mathrm{P}}^l$$

to approximate $H^1_{\mathrm{P}}(\Omega)$. Note the dimension of X_{P}^l is n_l^2 with $n_l = 2^l s$. Write

$$u^{\epsilon,l}(x, y) \in X_{\mathrm{P}}^l$$

as

$$u^{\epsilon,l}(x, y) = \sum_{i,j=0}^{2^l s - 1} u_{i,j}^{\epsilon,l} \phi_i^l(x) \phi_j^l(y),$$

and similarly, the boundary measure μ^l,

$$\mu^l(x, y) = \sum \mu_{i,j}^l \phi_i^l(x) \phi_j^l(y) \in X_{\mathrm{P}}^l,$$

where $\mu_{i,j}^l$ is calculated as in (3.23) in Sect. 3.2.

$$\begin{aligned} g^l(x, y) \quad &= \quad \sum_{pq} \left[\int g \phi_p^l \phi_q^l dxdy \right] \phi_p^l(x) \phi_q^l(y) \in X_{\mathrm{P}}^l \\ f^l(x, y) \quad &= \quad \sum_{pq} \left[\int f \phi_p^l(x) \phi_q^l(y) dxdy \right] \phi_p^l(x) \phi_q^l(y) \in X_{\mathrm{P}}^l. \end{aligned}$$

Table 1. The Relative Error in the L^2 norm of the Wavelet-Galerkin Penalty Solution for the Disk

Solution	Epsilon	Relative Error
u_1	$\epsilon = 1$	$E = 2.762 \times 10^{-4}$
	$\epsilon = 10^{-3}$	$E = 9.435 \times 10^{-5}$
	$\epsilon = 10^{-6}$	$E = 2.826 \times 10^{-6}$
	$\epsilon = 10^{-9}$	$E = 4.025 \times 10^{-8}$
	$\epsilon = 10^{-12}$	$E = 6.400 \times 10^{-8}$
u_2	$\epsilon = 1$	$E = 0.001001$
	$\epsilon = 10^{-3}$	$E = 3.219 \times 10^{-4}$
	$\epsilon = 10^{-6}$	$E = 1.052 \times 10^{-5}$
	$\epsilon = 10^{-9}$	$E = 1.739 \times 10^{-7}$
	$\epsilon = 10^{-12}$	$E = 1.901 \times 10^{-7}$
u_3	$\epsilon = 1$	$E = 0.06524$
	$\epsilon = 10^{-3}$	$E = 0.0274$
	$\epsilon = 10^{-6}$	$E = 8.747 \times 10^{-5}$
	$\epsilon = 10^{-9}$	$E = 9.405 \times 10^{-8}$
	$\epsilon = 10^{-12}$	$E = 6.451 \times 10^{-9}$

Table 2. The Relative Error in the L^2 norm of the Wavelet-Galerkin Penalty Solution for the Diamond

Solution	Epsilon	Relative Error
u_1	$\epsilon = 1$	$E = 2.522 \times 10^{-4}$
	$\epsilon = 10^{-3}$	$E = 7.926 \times 10^{-5}$
	$\epsilon = 10^{-6}$	$E = 3.052 \times 10^{-6}$
	$\epsilon = 10^{-9}$	$E = 1.492 \times 10^{-5}$
	$\epsilon = 10^{-12}$	$E = 1.354 \times 10^{-7}$
u_2	$\epsilon = 1$	$E = 0.001005$
	$\epsilon = 10^{-3}$	$E = 2.683 \times 10^{-4}$
	$\epsilon = 10^{-6}$	$E = 1.371 \times 10^{-5}$
	$\epsilon = 10^{-9}$	$E = 6.291 \times 10^{-5}$
	$\epsilon = 10^{-12}$	$E = 5.990 \times 10^{-7}$

Applying the Galerkin method to (4.2) (see, e.g., [6]), one obtains the following linear system.

$$A^l U^{\epsilon,l} + U^{\epsilon,l} + \frac{1}{\epsilon} M^l U^{\epsilon,l} = F^l + \frac{1}{\epsilon} M^l G^l,$$

where $U^{\epsilon,l}$, M^l, F^l, G^l are obtained through lexicographical ordering. Note that M^l is a diagonal matrix.

Proposition 4.2. *Suppose $u_\epsilon \in C^2(\omega)$ is a solution of* (4.2)*, and let u_ϵ^j be the wavelet-Galerkin approximation to u_ϵ, then*

$$\begin{aligned} \|u_\epsilon - u_\epsilon^j\|_{L^2(\omega)} &\leq C\left(\frac{1}{2^j}\right)^2 \\ \|u_\epsilon - u_\epsilon^j\|_{H^1(\omega)} &\leq C\left(\frac{1}{2^j}\right) \end{aligned}$$

Proof. See Theorem 4.1 in [15]. □

Remarks. The Wavelet-Galerkin approximation u_ϵ^j differs from the solution u of the original differential equation by an estimate of the following type:

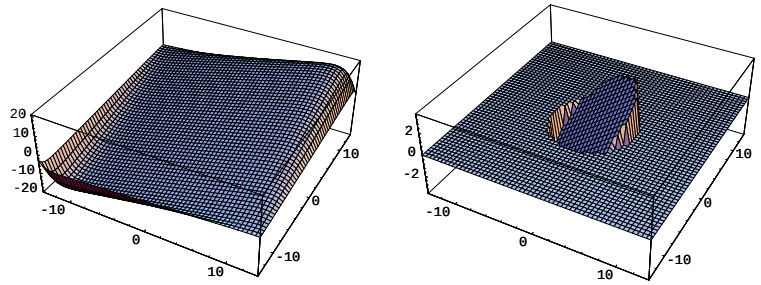

Fig. 1. The wavelet-Galerkin-penalty approximation for the exact solution $u = x + y$ on the disk for $\epsilon = 1$

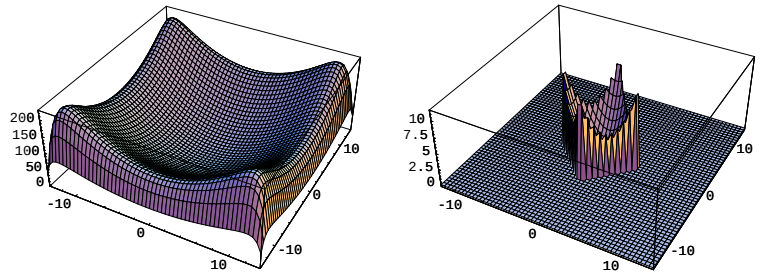

Fig. 2. The wavelet-Galerkin-penalty approximation for the exact solution $u = x^2 + y^2$ on the diamond for $\epsilon = 1$

$$\|u - u_\epsilon^j\|_{H^1(\omega)} = o(1) + O(2^{-j}).$$

These estimates do not depend on the order of the Daubechies wavelets used, but numerical evidence from a number of sources indicates there should be such a dependence and we would expect an estimate of the form

$$\|u - u_\epsilon^j\|_{H^1(\omega)} = 0(\epsilon) + O(2^{-(g-1)j}),$$

but we don't have a proof of this at this time.

4.4. Numerical experiments: the Dirichlet problem

In this section we want to describe a sequence of numerical experiments concerning the Dirichlet problem. Gaussian elimination for solving the resulting linear system was initially used. For this paper we concentrated on the feasibility of the wavelet representation for a very general boundary value problem. Finding efficient implementations are the next step and are being investigated. For instance, a proper iterative solver is currently under investigation for speeding up the process, and the Jacobi method seems to give promising results. In addition multiscale methods are being developed to improve the computational efficiency.

We report here on two different geometries and two different exact solutions. We choose a fictitious domain Ω and two solution domains ω_1 and ω_2.

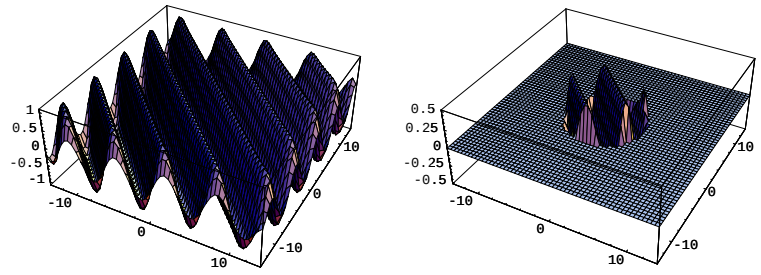

Fig. 3. The wavelet-Galerkin-penalty approximation for the exact solution $u = \sin(x + y)$ on the disk for $\epsilon = 1$

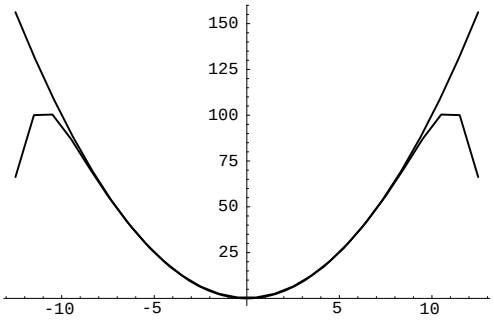

Fig. 4. The wavelet-Galerkin penalty approximation for $\epsilon = 1$ restricted to $y = 0$ compared to the exact solution $u = x^2 + y^2$ in the diamond

$$\begin{aligned} \Omega &= \{(x,y): \quad |x|,|y| < 15\} \\ \omega_1 &= \{(x,y): \quad x^2 + y^2 < 5^2\} \\ \omega_2 &= \{(x,y): \quad |x| + |y| < 5\} \end{aligned}$$

We consider the following exact solutions u_i of $-\Delta u_i + u_i = f_i$ with boundary data g_i, where

$$\begin{array}{llll} u_1 & = x + y, & f_1 = x + y, & g_1 = x + y \\ u_2 & = x^2 + y^2, & f_2 = x^2 + y^2 - 4, & g_2 = x^2 + y^2 \\ u_3 & = \sin(x + y), & f_3 = 3\sin(x + y), & g_3 = \sin(x + y) \end{array} \tag{4.12}$$

and restrict these functions to the boundary of the domains ω_1 and ω_2, and solve for the penalty-wavelet-Galerkin solution u_ϵ^j in each case. In these first experiments we only solve at level 0, and let ϵ vary. The results are tabulated in Tables 1 and 2 Here the relative error is of the form

$$E = \frac{\|u - u_\epsilon\|_{L^2(\omega)}}{\|u\|_{L^2(\omega)}}$$

In both tables we see that for this fixed "mesh size" (level 0, for wavelet length 5, corresponding to a basis of 35 translated scaling functions whose support intersects $[0, 30]$ on the horizontal axis, and similarly in the vertical axis), a point is reached

at which the errors stabilize (for this data at $\epsilon = 10^{-9}$ to 10^{-12}), and it would be necessary to go to a higher level to achieve greater accuracy.

In Fig. 1 we see the wavelet-Galerkin-penalty solution for the two exact solution $u = x+y$, and we see on the left the penalty solution in the full region $D = [-15, 15] \times [-15, 15]$ (here it is a box of the form $[-12.5, 12.5] \times [-12.5, 12.5]$, corresponding to all of the wavelets with support entirely in the box). In the right is the same approximate solution restricted to the geometric domain (in this case the disk of radius 5) on which we are solving the Dirichlet problem. In Fig. 2 we find corresponding approximations for the exact solutions $u = x^2 + y^2$ and $u = \sin(x + y)$ on the diamond and the disk, respectively. These are all plotted at level 1, with 56 points on a side. The corresponding figures for level 0 would have 26 points, and similarly for higher level. In Fig. 4 we find a comparison of a slice of the two-dimensional approximation with the slice of the corresponding exact solution. We see in this figure, which is calculated at level 0, that there is no discernible error in the figure in the Dirichlet problem region, that is for $r = \sqrt{x^2 + y^2} < 5$.

Acknowledgements. The authors would like to thank the following individuals for their useful comments during the preparation of this paper: Roland Glowinski, John Weiss, Tsorng-Whay Pan, Wayne Lawton, and Howard Resnikoff.

References

1. Beylkin G. (1992): On the representation of operators in bases of compactly supported wavelets. SIAM J. Numer. Anal. **6**(6): 1716–1740
2. Daubechies, I. (1988): Orthonormal bases of compactly supported wavelets. Comm. Pure Appl. Math. **41**, 906–966
3. Daubechies, I. (1992): Ten Lectures on Wavelets. CBMS-NSF Series in Applied Mathematics, SIAM Publications, Philadelphia
4. Federer, H. (1969): Geometric measure theory. Springer-Verlag, New York
5. Guisti, E. (1984): Minimal surfaces and functions of bounded variation. Birkhauser, Boston
6. Glowinski, R. (1984): Numerical methods for nonlinear variational problems. Springer Series in Computational Physics, Springer-Verlag, New York
7. Glowinski, R., Lawton, W., Ravachol, M., Tenenbaum, E. (1990): Wavelet solution of linear and nonlinear elliptic, parabolic and hyperbolic problems in one dimension. In: Glowinski, R., Lichnewski, A. (eds.) Proceedings of the Ninth International Conference on Computing Methods in Applied Sciences and Engineering, Philadelphia, SIAM
8. Glowinski, R., Pan, T.W., Wells, R.O.Jr., Zhou, X. (1992): Wavelet solutions for the Neumann problem. Technical Report 92-01, Rice University, Computational Mathematics Laboratory
9. Heller, P., Resnikoff, H.L., Wells, R.O.Jr. (1992): Wavelet matrices and the representation of discrete functions. In: Chui, C. (ed.) Wavelets: a tutorial. Academic Press, Cambridge, MA, 15–50
10. Latto, A., Resnikoff, H.L, Tenenbaum, E. (1991): The evaluation of connection coefficients of compactly supported wavelets. In: Proceedings of the USA-French Workshop on Wavelets and Turbulence. Princeton University (to appear) 1995
11. Lawton W., Morrell, W., Tenenbaum, E., Weiss, J. (1990): The wavelet-Galerkin method for partial differential equations. Technical Report AD901220, Aware Inc.
12. Mallat, S., Hwang, W.L. (1991): Singularity detection and processing with wavelets. Technical Report 549, New York University, Courant Institute of Mathematical Sciences
13. Resnikoff, H.L., Wells, R.O.Jr. (1992): Wavelet analysis and the geometry of Euclidean domains. J. Geom. Phys. **8**, 273–282
14. Weiss, J. (1991): Wavelets and the study of two dimensional turbulence. In: Proceedings of the USA-French Workshop on Wavelets and Turbulence. Princeton University (to appear)

15. Wells, R.O.Jr., Zhou, X. (1994): Wavelet interpolation and approximate solutions of elliptic partial differential equations. In: Wilson, R., Tanner, E.A. (eds.) Noncompact Lie Groups. Kluwer (to appear). Proceedings of NATO Advanced Research Workshop, pp. 349–366

This article was processed by the author using the LaTeX style file *pljour1* from Springer-Verlag.